European Journal of Medicinal Chemistry 45 (2010) 6027–6038

Contents lists available at ScienceDirect

European Journal of Medicinal Chemistry

journal homepage: http://www.elsevier.com/locate/ejmech

Original article

Synthesis and biological evaluation of some thiazolylpyrazole derivatives as dual anti-inflammatory antimicrobial agents

Adnan A. Bekhit [a,*], Hesham T.Y. Fahmy [b], Sherif A.F. Rostom [a,c], Alaa El-Din A. Bekhit [d]

[a] Department of Pharmaceutical Chemistry, Faculty of Pharmacy, Alexandria University, Alexandria 21521, Egypt
[b] Department of Pharmaceutical Sciences, College of Pharmacy, South Dakota State University, Box 2202C, Brookings, SD 57007, USA
[c] Department of Pharmaceutical Chemistry, Faculty of Pharmacy, King Abdulaziz University, P.O. 80260, Jeddah 21589, Saudi Arabia
[d] Food Science, Otago University, Dunedin, New Zealand

ARTICLE INFO

Article history:
Received 6 July 2010
Received in revised form
14 September 2010
Accepted 1 October 2010
Available online 20 October 2010

Keywords:
Thiazolylpyrazoles
anti-Inflammatory activity
COX inhibitory activity
Acute toxicity
Ulcerogenic effect
Antimicrobial activity

ABSTRACT

The synthesis of a novel series of 4-thiazolylpyrazolyl derivatives is described in the present report. All the newly synthesized compounds were examined for their anti-inflammatory activity using cotton pellet-induced granuloma and carrageenan-induced rat paw edema bioassays. Their inhibitory activities of cyclooxygenase-1 and cyclooxygenase-2 (COX-1 and COX-2), ulcerogenic effect and acute toxicity were also determined. Furthermore, all compounds were evaluated for their *in vitro* antimicrobial activity against *Escherichia coli, Staphylococcus aureus* and *Candida albicans*. A docking pose for compounds **8b**, **10a** and **10b** separately in the active site of the human COX-2 enzyme and DNA-gyrase B was also obtained. The results revealed that compounds **8b**, **10a** and **10b** exhibited good anti-inflammatory activity with no or minimal ulcerogenic effect and good safety margin. Compounds **10a** and **10b** were found to be the most potent anti-inflammatory agents in the present study. Meanwhile, **10a** and **10b** displayed higher selective inhibitory activity towards COX-2 compared to indomethacin. Moreover, compounds **10a** and **10b** exhibited promising antibacterial against both *E. coli* and *S. aureus*. Docking studies for **8b**, **10a** and **10b** with COX-2 (PDB ID: 1CX2) and DNA-gyrase B (PDB ID: 1EI1) showed good binding profile.

1. Introduction

Non-steroidal anti-inflammatory drugs (NSAIDs) have been recognized as important therapeutic agents for the treatment of rheumatoid arthritis and its variants. However, large doses of NSAIDs or long term use usually results in gastrointestinal mucosal damage, intolerance and renal toxicity [1–4]. Despite the efforts that had been made to improve the pharmacological profile of NSAIDs, ulcerogenicity remains the most limiting problem in their clinical use. A major breakthrough in anti-inflammatory research occurred when it was discovered that COX exists in three isoforms COX-1, COX-2 and COX-3 which are regulated differently [5,6]. The discovery of the inducible isoform COX-2 spurred the search for novel anti-inflammatory agents devoid of the undesirable effects associated with classical non selective NSAIDs. Consequently, a new generation of COX-2 selective inhibitors has been clinically used with the hope that they would exhibit a reduced risk in gastrointestinal events. Among this class of compounds, celecoxib; 4-[5-(4-methylphenyl)-3-(trifluoromethyl)-1*H*-pyrazol-1-yl]benzene-sulfonamide (Fig. 1) was shown to be a potent and a gastrointestinal safe anti-inflammatory and analgesic agent. Celecoxib is considered a typical model of pyrazole containing diaryl heterocyclic template that is known to inhibit COX-2 selectively [7]. Moreover, several other compounds containing pyrazole functionality were also reported to exhibit anti-inflammatory activity [8–12]. Furthermore, much attention has been focused on pyrazoles as antimicrobial agents after the discovery of the natural pyrazole C-glycoside pyrazofurin; 4-hydroxy-3-β-D-ribofuranosyl-1*H*-pyrazole-5-carboxamide (Fig. 1) which demonstrated a broad spectrum of antimicrobial activities [13,14]. This led to the synthesis of several pyrazole derivatives that exhibited antimicrobial activity by Tanitame and coworkers [15–17].

Co-administration of multiple drugs for treatment of inflammatory conditions associated with microbial infection is a major risk especially in the case of patients with impaired liver or kidney functions. A mono therapy of a drug with dual anti-inflammatory antimicrobial activity would be preferred from the pharmacoeconomic and patient compliance point of view. This premise was one of the goals of our research program aimed at the discovery of new pyrazoles that would possess dual anti-inflammatory antimicrobial activities [18–29]. Some of our reported pyrazolyl compounds [18–28] showed pronounced dual activities. Four of these lead

* Corresponding author. Tel.: +20 3 4871317; fax: +20 3 4873273.
E-mail address: adnbekhit@hotmail.com (A.A. Bekhit).

0223-5234/$ – see front matter © 2010 Elsevier Masson SAS. All rights reserved.
doi:10.1016/j.ejmech.2010.10.001

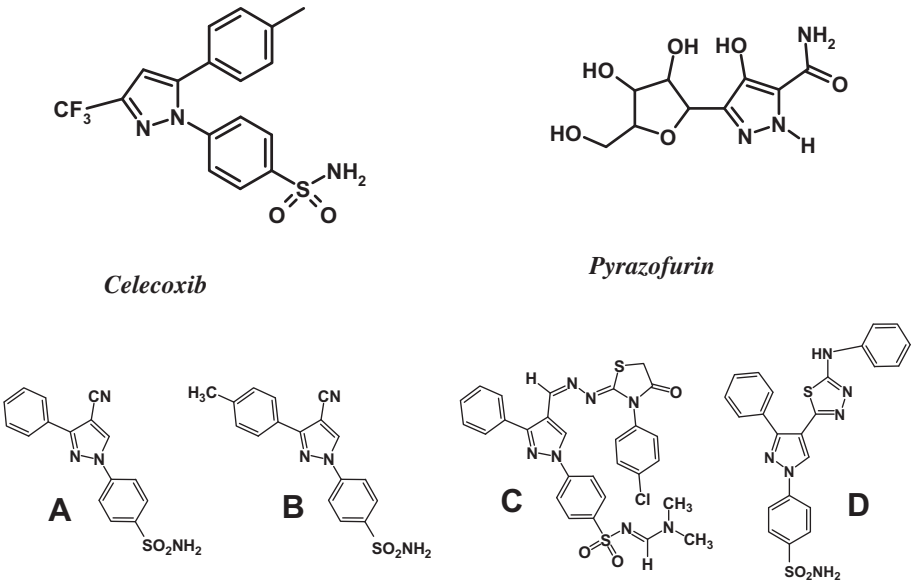

Fig. 1. Structures of celecoxib and reported active pyrazole derivatives **A**, **B**, **C** and **D**.

compounds **A** [26], **B** [26] **C** [27] and **D** [28] displayed appreciable anti-inflammatory and selective COX-2 inhibitory activity (Fig. 1). On the other hand, thiazole derivatives were reported to possess antimicrobial [20,30] or anti-inflammatory [20,31] activities. Encouraged by these results it was decided to synthesize novel compounds having essentially in their structure the pyrazole counterpart linked to different thiazole derivatives in order to investigate the effects of such molecular variation on the anti-inflammatory antimicrobial activity. This type of molecular variation could regulate other biological functions; therefore the new compounds were investigated for their inhibitory activities of COX-1 and COX-2 enzymes. A docking pose of the most active compounds separately in the active site of the human COX-2 enzyme and DNA-gyrase B was also obtained. Additionally, the ulcerogenic effect and acute toxicity profiles of the active compounds were determined.

2. Chemistry

Synthesis of the intermediate and target compounds was performed according to the reactions illustrated in Scheme 1. The intermediates 3-aryl-1-phenyl-1*H*-pyrazole-4-aldoxime **2a**,**b** were obtained in good yields by the condensation of 3-aryl-1-phenyl-1*H*-pyrazole-4-carboxaldehyde [32] **1a**,**b** with hydroxylamine hydrochloride in ethanol containing anhydrous sodium acetate. ^{1}H NMR spectra of these compounds revealed a singlet characteristic for hydroxyl group proton at $\delta = 11.87-11.91$ ppm and iminomethyl proton at $\delta = 7.42-7.46$ ppm confirming existence of these compounds as E-isomers [33]. Dehydration of the oximes **2a**,**b** with acetic anhydride [26] afforded the cyano derivatives **3a**,**b**. The IR spectra for **3a**,**b** showed the specific band for the cyano group at 2228–2232 cm^{-1}.Cyclization of the cyano derivatives **3a**,**b** with cysteamine hydrochloride in the presence of sodium hydroxide resulted in thiazolidine derivatives **4a**,**b** [34]. ^{1}H NMR spectra of thiazolidine **4a**,**b** showed a two triplets assigned for SCH_2 and NCH_2 protons at $\delta = 3.34-3.37$ ppm and $\delta = 4.46-4.48$ ppm, respectively. Condensation of the aldehydes **1a**,**b** with 4-fluorobenzylamine gave rise to Schiff's bases **5a**,**b**. ^{1}H NMR spectra of these compounds revealed a singlet characteristic for iminomethyl proton at $\delta = 7.42-7.46$ ppm confirming the existence of these compounds as E-isomers [33]. Reaction of **5a**,**b** with thioglycolic acid in the presence of anhydrous zinc chloride resulted in the thiazolidinone derivatives **6a**,**b**. ^{1}H NMR spectra of these compounds revealed double doublet and singlet at $\delta = 3.68-3.71$ ppm and at $\delta = 5.62-5.68$ ppm which are characteristics for methylene and methine protons of thiazolidinone ring, respectively. Heating, under reflux, a solution of pyrazole carboxaldehyde **1a**,**b** and L-cysteine in aqueous ethanol [35], followed by N-protection [36], using $(Boc)_2O$ resulted in compounds **7a**,**b**. These compounds **7a**,**b** either subjected to *N*-deprotection using 4 N HCl/dioxane leading to thiazolidine carboxylic acid derivatives **8a**,**b** or allowed to react with NH_4OH in the presence of DCC/HOBt to afford the corresponding carboxamide derivatives **9a**,**b**. The latter when subjected to N-deprotection resulted in carboxamide derivatives **10a**,**b**. It is worth mentioning that all trials to separate diastereomers of compounds **7**, **8**, **9** and **10** went in vain. In 2,4-disubstituted thiazolidines, the *cis* and *trans* diastereomers freely interconverted in solution [37]. The ratio of diastereomers observed for the compounds in the present study was 1:1 based on ^{1}H NMR spectroscopy. Diastereomerization was at the C-2 center via an iminium intermediate [35]. This property prevents the independent examination of the biological activities of the two diastereomers; hence the structure was drawn and discussed throughout this paper as diastereomeric mixture.

3. Results and discussion

3.1. Anti-inflammatory activity

3.1.1. Cotton pellet-induced granuloma bioassay

The anti-inflammatory activities of the target compounds **4a**,**b**, **6a**,**b**, **8a**,**b** and **10a**,**b** were evaluated by applying the cotton pellet-induced granuloma bioassay in rats as described earlier [38] using indomethacin and celecoxib as reference standards. The ED_{50} value for each of the test compounds was expressed as the mean ± SEM. Significant difference between the control and treated groups was estimated using one way analysis of variance (ANOVA) and the significance of the difference between means was determined by Tukey's test at $P < 0.001$ (Table 1). Three of the test compounds **8b**, **10a** and **10b** possessed anti-inflammatory activity ($ED_{50} = 9.74$, 8.11 and 7.86 μmol, respectively) surpassing that of indomethacin and celecoxib ($ED_{50} = 9.64$ and 16.74 μmol, respectively). The results

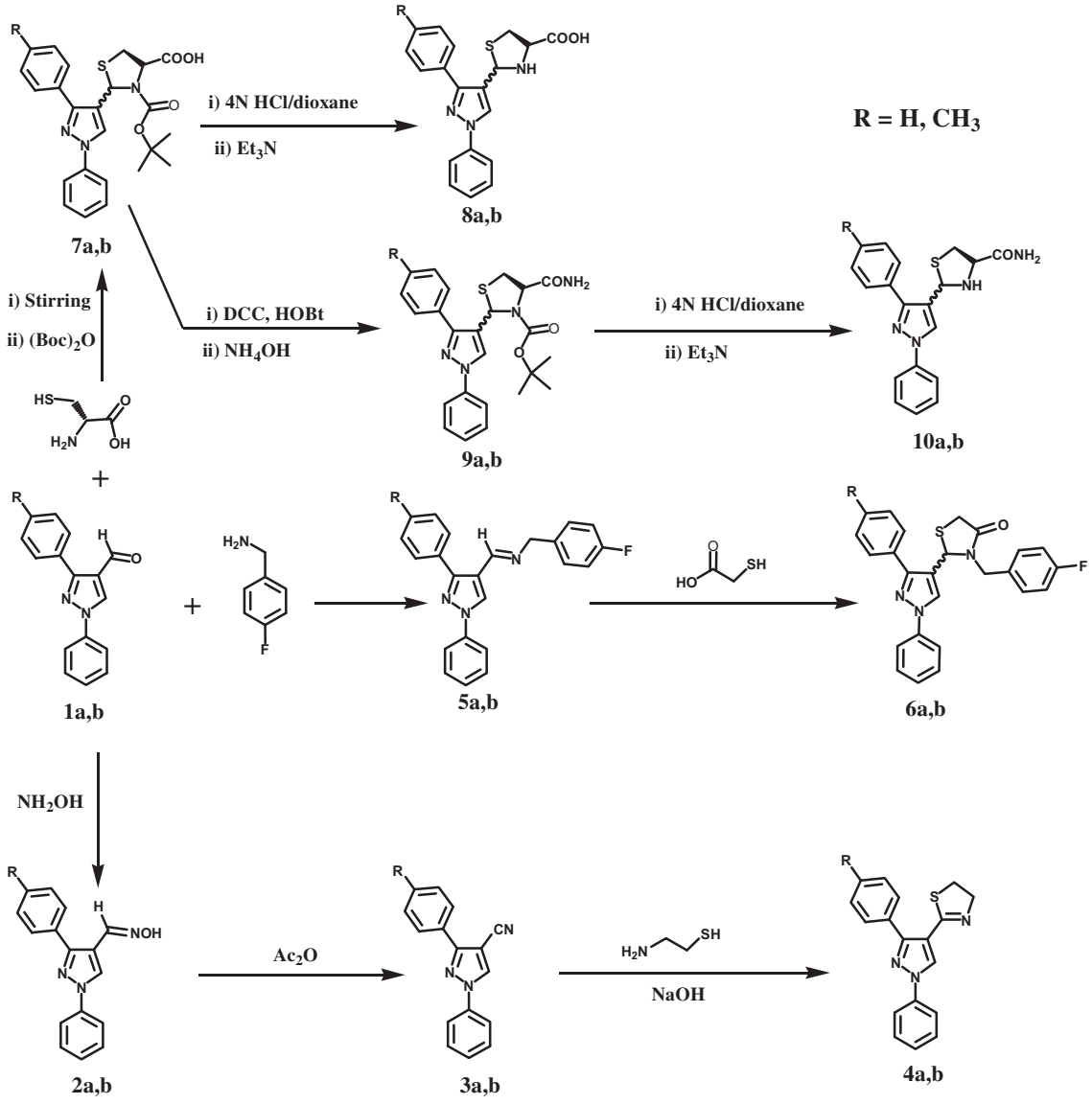

Scheme 1.

revealed that thiazolidine carboxamide derivatives **10a**,**b** and thiazolidine carboxylic acid derivative **8a**,**b** appeared to possess higher anti-inflammatory activity than thiazolidine derivatives **4a**,**b** or thiazolidinone **6a**,**b**. Within thiazolidine derivatives **8a**,**b** and **10a**,**b**, compounds **8b**, **10b** (ED_{50} = 9.74 and 7.86 μmol, respectively) containing *p*-tolyl substitution were more active than compounds **8a**, **10a** (ED_{50} = 11.86 and 8.11 μmol, respectively) which contained phenyl substitution. This may affect the structure conformation to have hydrogen bonding with the backbone of COX-2 enzyme as will be discussed in the docking section. Compound **10b** was proved to be the most potent anti-inflammatory agent (ED_{50} = 7.86 μmol) whereas compound **6b** (ED_{50} = 28.42 μmol) was found to be the least active as anti-inflammatory agent (Table 1).

Table 1
The anti-inflammatory activity (ED_{50}, μmol/cotton pellet) and ulcerogenic activity.

Test Compound	ED_{50} (μmol)	% Ulceration
Control	–	100^{z}
Indomethacin	9.64 ± 0.28^{t}	100^{z}
Celecoxib	16.74 ± 0.22^{v}	0.0^{x}
4a	22.37 ± 0.18^{w}	ND[a]
4b	26.62 ± 0.24^{y}	ND
6a	25.08 ± 0.44^{x}	ND
6b	28.42 ± 0.32^{z}	ND
8a	11.86 ± 0.34^{u}	ND
8b	9.74 ± 0.38^{t}	70^{y}
10a	8.11 ± 0.15^{s}	0.0^{x}
10b	7.86 ± 0.14^{r}	0.0^{x}

[r–z]Means within each activity with different superscripts are significantly different from control ($P < 0.001$).
[a] ND = Not determined.

3.1.2. Carrageenan-induced rat paw edema bioassay

Compounds showing promising anti-inflammatory activity in the cotton pellet-induced granuloma bioassay (**8b**, **10a** and **10b**) were further evaluated for their *in vivo* systemic effect using carrageenan-induced paw edema bioassay in rats [39]. The results showed that compounds **8b**, **10a** and **10b** displayed systemic anti-inflammatory activity (% protection = 78.4 and 79.4, 82.5, respectively) comparable or slightly higher than celecoxib (% protection = 77.3) but higher than indomethacin (% protection = 73.2). Thiazolidine derivative **10b**

Table 2
Effect of compounds **8b**, **10a** and **10b** on carrageenan-induced rat paw edema (ml), % protection and activity relative to indomethacin.

Test compound	Increase in paw edema (ml) ± SEM[a,b]	% Protection	Activity relative to indomethacin
Control	0.97 ± 0.028	0.0	0.0
Indomethacin	0.26 ± 0.024	73.2	100
Celecoxib	0.22 ± 0.014	77.3	105.60
8b	0.21 ± 0.016	78.4	107.10
10a	0.20 ± 0.026	79.4	108.46
10b	0.17 ± 0.018	82.5	112.70

[a] SEM denotes the standard error of the mean.
[b] All data are significantly different from control ($P < 0.001$).

containing *p*-tolyl substitution also showed higher activity than compound **10b** containing phenyl substitution in this assay (Table 2).

3.1.3. Human COX-1 and COX-2 enzymatic activity

Compounds **8b**, **10a** and **10b** that showed potent anti-inflammatory profiles in animal models were further tested for their ability to inhibit human COX-1 and COX-2 enzymes *in vitro* as described by Wakitani et al. [40]. COX-1 assay was carried out using platelets microsome fraction. Human platelets were prepared from NSAID-free normal human volunteers according to the method of Hammarström and Falardeau [41]. COX-2 assay was performed using human recombinant COX-2 purchased from Sigma–Aldrich. The inhibitory activity was expressed as the concentration of the compound causing 50% enzyme inhibition (IC_{50} μmol) (Table 3). The results revealed that the test compounds exhibited weak inhibitory activity against COX-1 enzyme (IC_{50} values ranged between 96.22 and >100 μmol) compared with indomethacin ($IC_{50} = 0.26$ μmol), however compound **8b** (IC50 = 96.22 μmol) was more potent than celecoxib ($IC_{50} = > 100$ μmol). The test compounds showed higher inhibitory profile against COX-2 (IC_{50} values between 0.38 and 0.94 μmol) compared with indomethacin ($IC_{50} = 2.63$ μmol). All test compounds showed approximate selectivity ratio (COX-1/COX-2) lower than that of celecoxib. In general, the results revealed that compounds having thiazolidine carboxamide moiety (compounds **10a** and **10b**) possessed higher selectivity towards COX-2 enzyme than compound containing thiazolidine carboxylic acid moiety (compound **8b**). However, within thiazolidine carboxamide class of compounds, the selective COX-2 inhibition of the tolyl derivative **10b** was greater than the phenyl derivative **10a**. Compounds **10a** and **10b**, the most selective COX-2 inhibitors in the present study (approximate selectivity ratio = 212.77 and 263.16, respectively), had lower selectivity compared to celecoxib (approximate selectivity ratio > 333).

3.1.4. Ulcerogenic effect

The most active compounds **8b**, **10a** and **10b** were evaluated for their ulcerogenic potential in rats [42]. Thiazolidine carboxamide derivatives **10a**,**b** proved to have superior gastrointestinal safety profiles (0.0% ulceration) in the population of test animals at oral doses of 30 μmol/kg per day, compared to indomethacin, the reference drug, which was found to cause 100% ulceration under the same experimental conditions (Table 1). Thiazolidine carboxylic acid derivative **8b** showed a significant ulcerogenic effect (70%), however this was lower than that of indomethacin. Gross observation of the isolated rat stomachs showed a normal stomach texture for compounds **10a**,**b**.

Table 3
In vitro human COX-2[a] and COX-1[b] enzymes inhibitory activities of compounds **8b**, **10a** and **10b**.

Test compound	COX-2 IC_{50} (μM)[c]	COX-1 IC_{50} (μM)[c]	Approximate selectivity ratio
			COX-1/COX-2
Indomethacin	2.63 ± 0.02	0.26 ± 0.32	0.098
Celecoxib	<0.3	>100	>333
8b	0.94 ± 0.02	96.22 ± 0.24	102.13
10a	0.47 ± 0.05	>100	>212.77
10b	0.38 ± 0.06	>100	>263.16

[a] Human recombinant COX-2 enzyme.
[b] Human COX-1 enzyme from human platelets.
[c] Values are means of at least four independent experiments.

3.1.5. Acute toxicity

Compounds **8b**, **10a** and **10b** were further evaluated for their oral acute toxicity in male mice using a previously reported method [43]. The results indicated that the test compounds proved to be non-toxic and well tolerated by experimental animals up to 150 mg/kg. Moreover, these compounds were tested for their toxicity through the parenteral route [20]. The results revealed that all test compounds were non-toxic up to 80 mg/kg.

3.1.6. Docking studies

Molecular docking studies of compound **8b**, **10a** and **10b** were performed using Molecular Operating Environment (MOE-Dock 2006) module [44] in order to rationalize the obtained biological results. Molecular docking studies further helps in understanding the various interactions between the ligand and enzyme active site in detail.

The determination of the three-dimensional co-crystal structure of COX-2 complex with a selective inhibitor, **SC-558** (Fig. 2; PDB ID: 1CX2) has led to the development of a model for the topography of the NSAIDs binding site in human COX-2 [45]. Therefore, herein we performed the docking studies using this COX-2 co-crystal structure with **SC-558** as a template.

Figs. 3–5 show the binding interactions of compounds **8b**, **10b** and **10b** to the active site of COX-2, respectively, where they exhibited some similar interactions as with **SC-558**. Compound **8b** displayed hydrogen bond interaction with Tyr 385, in addition to hydrophobic interactions with His 90, Val 349, Leu 352, Ser 353, Leu 359, Arg 513, Phe 518 and Val 523. On the other hand, compound **10a** showed hydrogen bond interactions with Leu 352 and Ser 353, in addition to hydrophobic interactions with His 90, Arg 120, Val 349, Leu 352, Ser 353, Tyr 355, Tyr 385, Val 523 and Ala 527. Compound **10b** displayed hydrogen bond interactions with Tyr 355 and Arg 513, in addition to hydrophobic interactions with His 90, Val 116, Arg 120, Val 349, Leu 352, Ser 353, Tyr 355, Arg 513, Val 523, Gly 526, Ala 527 and Leu 531.

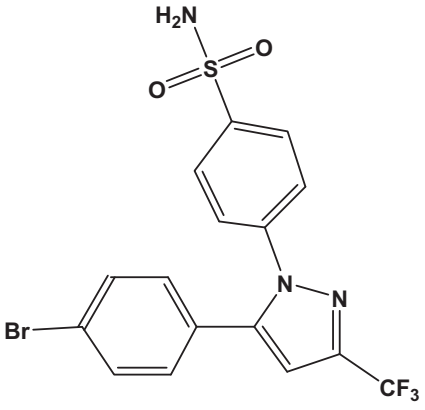

Fig. 2. Structure of **SC-558**.

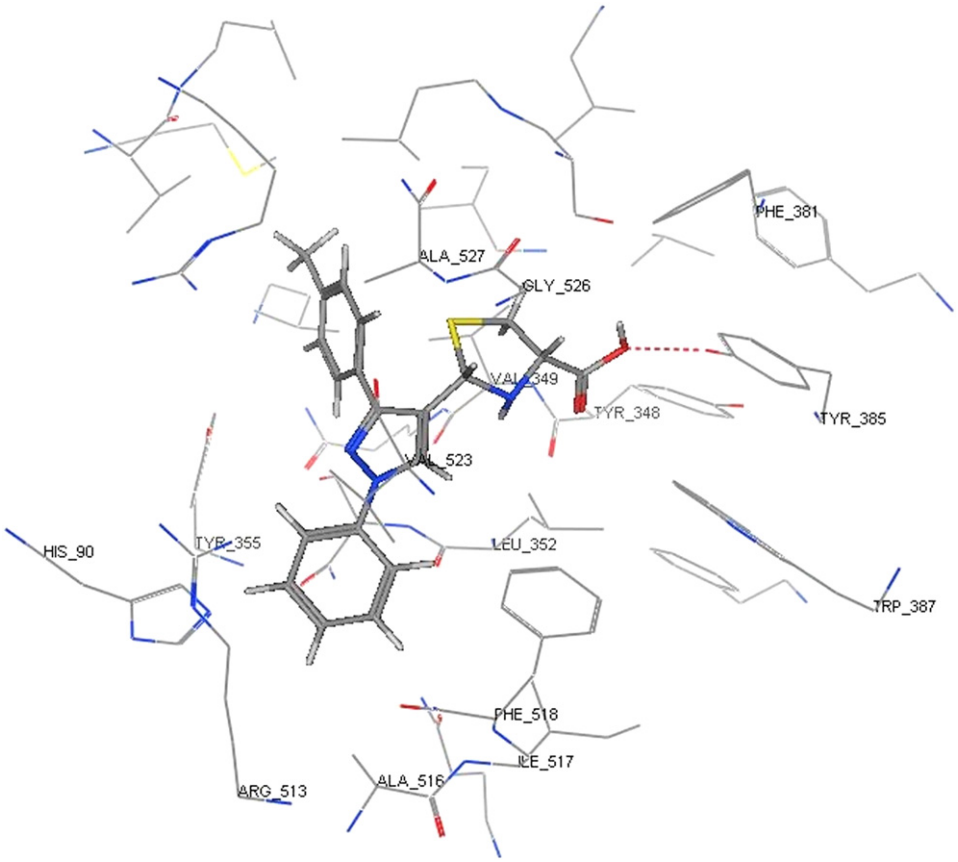

Fig. 3. 3D View from a molecular modeling study, of the minimum-energy structure of the complex of **8b** docked in COX-2 (PDB ID: 1CX2). Viewed using Molecular Operating Environment (MOE) module.

3.1.7. Antimicrobial activity

The designed compounds **4a**,**b**; **6a**,**b**; **8a**,**b** and **10a**,**b** were evaluated for their *in vitro* antimicrobial activity against *E. coli* ATCC 25922, as an example of Gram-negative bacteria, *S. aureus* ATCC 19433 as an example of Gram-positive bacteria, and *C. albicans* as a representative of fungi. The micro-dilution susceptibility test in Müller-Hinton Broth (Oxoid) and Sabouraud liquid Medium (Oxoid) were used for the determination of antibacterial and antifungal activities [46]. The minimal inhibitory concentration (MIC; μg/ml) of the test compounds are shown in Table 4. The results revealed that some of the newly synthesized compounds exhibited appreciable antibacterial activity. Thiazoline derivatives **4a**,**b** and thiazolidinone derivatives **6a**,**b** did not show appreciable antimicrobial activity. Compounds **8a**, **8b** and **10a** exhibited antibacterial activity against *E. coli* (MIC = 25 μg/ml) comparable to ampicillin, whereas compound **10b** (MIC = 12.5 μg/ml) showed two fold the antibacterial activity of ampicillin. Both compounds **10a** and **10b** (MIC = 12.5 μg/ml) exhibited antibacterial activity against *S. aureus* comparable to ampicillin. However, none of the screened compounds showed significant activity against *C. albicans* (MIC values >200) compared with the reference antifungal agent clotrimazole (MIC 12.5 μg/ml).

In a trial to study the antimicrobial mechanism of the most active thiazolidine carboxamide **10a**,**b**; the compounds were tested for their inhibition of DNA-gyrase [47] (full data will be published elsewhere). Compounds **10a** and **10b** showed promising DNA gyrase inhibitory activity, with IC_{50} of 5 μg/ml and 2.5 μg/ml respectively. Furthermore, we performed the docking studies of **10a** and **10b** with DNA-gyrase B (PDB ID: 1EI1). Figs. 6 and 7 show the binding interactions of compounds **10a** and **10b** to the active site of DNA-gyrase. Compound **10a** showed a hydrogen bond donor interaction with Asn 46, a hydrogen bond acceptor interaction with Val 118, and hydrophobic interactions with Asp 73, Ile 78, Pro 79, Ile 94, Gly 117, Val 118, Glt 119, Val 120 and thr 1165. Compound **10b** displayed 2 hydrogen bonds donor and one hydrogen bond acceptor interaction with Tyr 109, in addition to hydrophobic interactions with Glu 50, Asp 73, Arg 76, Gly 77, Ile 78, Gly 102, Lys 103, Ser 108, Tyr 109, Gly 117, Val 118, Gly 119, Val 120 and Thr 165.

The docking results showed that compound **10b** had better interactions with the backbone of DNA-gyrase enzyme than compound **10a**.

4. Conclusion

Compounds **8b**, **10a** and **10b** exhibited good anti-inflammatory activity with no or minimal ulcerogenic effect and good safety margin. Compounds **10a** and **10b** were found to be the most potent anti-inflammatory agents in the present study. Meanwhile **10a** and **10b** displayed higher selective inhibitory activity towards COX-2 compared to indomethacin. Moreover, compounds **10a** and **10b** exhibited promising antibacterial against both *E. coli* and *S. aureus*. Docking studies for both **10a** and **10b** with COX-2 (PDB ID: 1CX2) and DNA-gyrase B (PDB ID: 1EI1) showed good binding profile. Therefore, compounds **10a** and **10b** would represent a fruitful matrix for the development of a new class of dual anti-inflammatory antimicrobial agents that would deserve further investigation and derivatization.

It is worth mentioning that compounds **10a** and **10b** displayed anti-inflammatory profile comparable to our previously reported

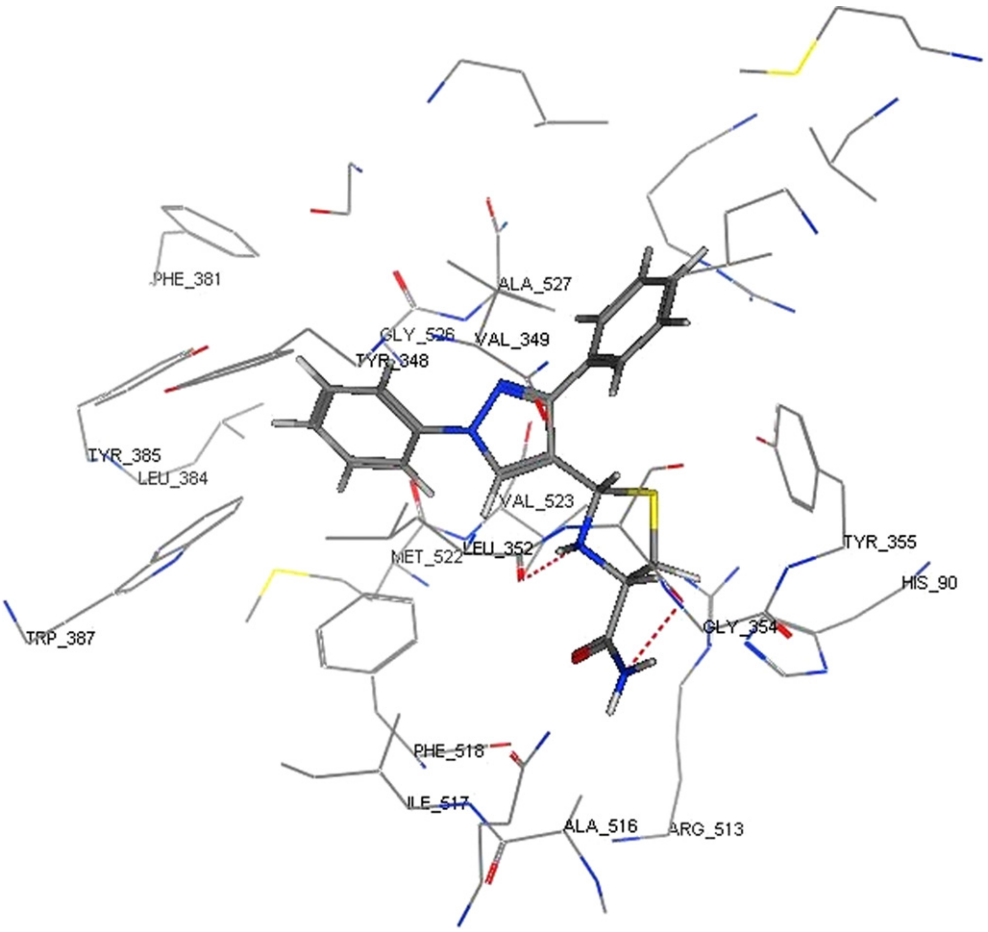

Fig. 4. 3D View from a molecular modeling study, of the minimum-energy structure of the complex of **10a** docked in COX-2 (PDB ID: 1CX2). Viewed using Molecular Operating Environment (MOE) module.

pyrazolyl benzenesulfonamide compounds **A** [26], **B** [26] and **C** [27]. However, the selective COX-2 inhibitory activity of compounds **10a** and **10b** was higher than those found with compounds **A**, **B** and **C**.

5. Experimental

5.1. Chemistry

Melting points were determined in open glass capillaries using Thomas Capillary melting point apparatus and are uncorrected. Infrared (IR) spectra were recorded using KBr discs on Perkin–Elmer 1430 infrared spectrophotometer. ^{1}H NMR spectra were scanned on Jeol-400 MHz Spectrometer, and chemical shifts are given in δ (ppm) downfield from tetramethylsilane (TMS) as internal standard. Splitting patterns were designated as follows; s: singlet; d: doublet; t: triplet; m: multiplet. Elemental analyses were performed on Vario El Fab.-Nr. elemental analyzer, Faculty of Pharmacy, Assiut University, Assiut, Egypt and were found to be within ±0.4% of the theoretical values. Follow up of the reactions and checking the purity of the compounds was made by thin layer chromatography (TLC) on silica gel-precoated aluminium sheets (Type 60 GF_{254} Merck) and the spots were detected by exposure to UV lamp at λ_{254} nm for few seconds.

5.1.1. 3-Aryl-1-phenyl-1H-pyrazole-4-aldoxime (**2a**,**b**)

A solution of the selected aldehyde **1a**,**b** (6.1 mmol), hydroxylamine hydrochloride (0.42g, 6.1 mmol) and anhydrous sodium acetate (0.5 g, 6.1 mmol) in ethanol (15 ml) was heated under reflux for 4 h. The reaction mixture was concentrated and left to attain room temperature. The separated solid product was filtered, washed with water, dried and crystallized from an appropriate solvent (Table 5).

IR (cm^{-1}), **2a**: 3378 (OH), 1647, 1596 (C=N). IR (cm^{-1}). ^{1}H NMR ($CDCl_3$), **2a**: δ 7.42 (s, 1H, N=CH), 7.48–7.69 (m, 10H, phenyl-H), 8.91 (s, 1H, pyrazole-C_5 H), 11.87 (s, 1H, OH, D_2O exchangeable). ^{13}C NMR ($CDCl_3$), **2a**: δ 33.1, 56.4, 106.5, 120.4, 126.7, 127.8, 128.7, 129.2, 129.6, 130.4, 133.2, 139.8, 151.1, 164.1.

IR (cm^{-1}), **2b**: 3369 (OH), 1643, 1595 (C=N). ^{1}H NMR ($CDCl_3$), **2b**: δ 2.36 (s, 3H, CH_3), 7.45 (s, 1H, N=CH), 7.49–7.58 (m, 5H, phenyl-H), 7.73 (d, 2H, J = 7.78 Hz, tolyl-$C_{3,5}$H), 7.82 (d, 2H, J = 7.78 Hz, tolyl-$C_{2,6}$H) 8.90 (s, 1H, pyrazole-C_5 H), 11.86 (s, 1H, OH, D_2O exchangeable). ^{13}C NMR ($CDCl_3$), **2b**: δ 24.6, 33.2, 56.2, 106.4, 120.6, 126.5, 127.5, 129.1, 129.7, 130.1, 130.5, 138.5, 139.7, 151.3, 164.4.

5.1.2. 3-Aryl-1-phenyl-1H-pyrazole-4-carbonitrile (**3a**,**b**)

A solution of the selected oxime **2a**,**b** (5.85 mmol) in acetic anhydride (10 ml) was heated under reflux for 3 h and the reaction mixture was then left over night at room temperature. The separated solid product was filtered, washed with water, dried and crystallized from an appropriate solvent (Table 5).

IR (cm^{-1}), **3a**: 2232 (CN), 1638 (C=N). IR (cm^{-1}). ^{1}H NMR ($CDCl_3$), **3a**: δ 7.33–7.73 (m, 10H, phenyl-H), 8.87 (s, 1H, pyrazole-C_5 H).

IR (cm^{-1}), **3b**: 2228 (CN), 1642 (C=N). ^{1}H NMR ($CDCl_3$), **3b**: δ 2.36 (s, 3H, CH_3), 7.31–7.58 (m, 5H, phenyl-H), 7.73 (d, 2H, J = 7.78 Hz, tolyl-$C_{3,5}$H), 7.82 (d, 2H, J = 7.78 Hz, tolyl-$C_{2,6}$H), 8.9 (s, 1H, pyrazole-C_5 H).

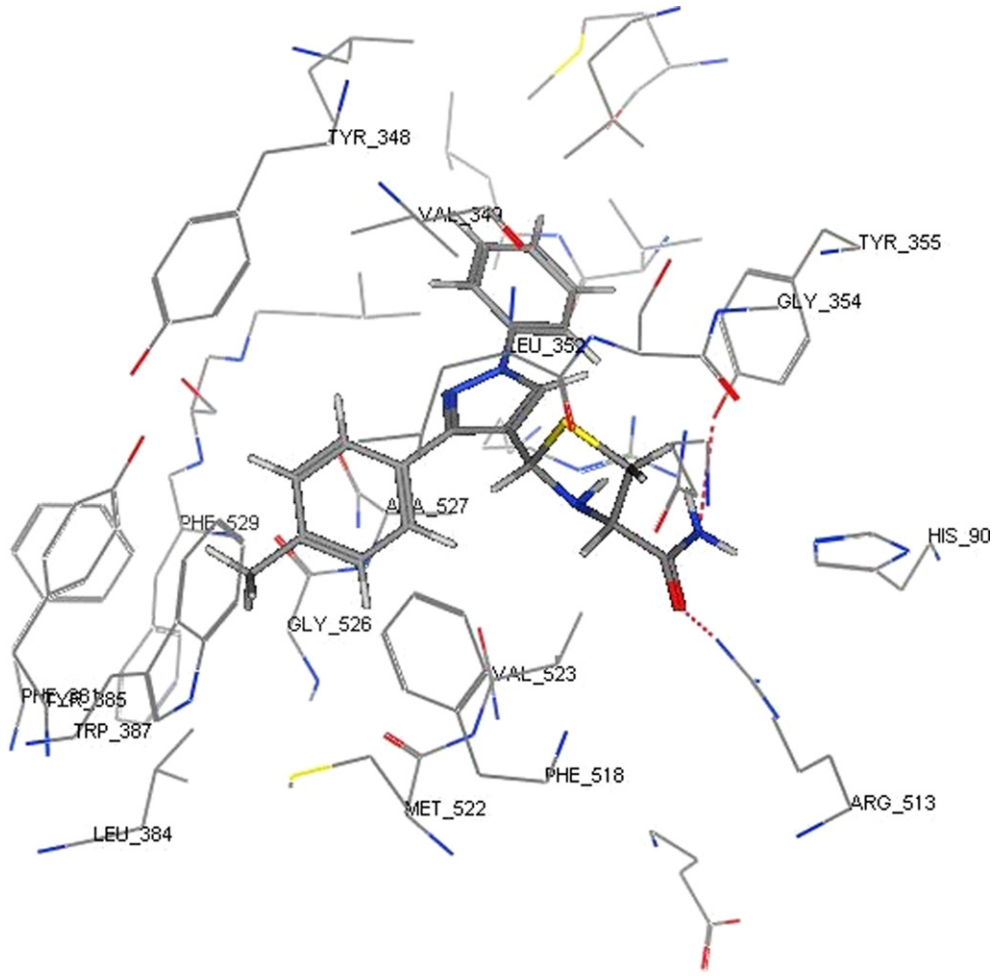

Fig. 5. 3D View from a molecular modeling study, of the minimum-energy structure of the complex of **10b** docked in COX-2 (PDB ID: 1CX2). Viewed using Molecular Operating Environment (MOE) module.

*5.1.3. 2-(3-Aryl-1-phenyl-1H-pyrazole-4-yl)-4,5-dihydrothiazole (**4a**,**b**)*

A 10 ml of 1 N NaOH was added to a solution of the selected nitrile **3a**,**b** (10 mmol) and cysteamine hydrochloride (2.25 g, 10 mmol) in ethanol (20 ml). The reaction mixture was heated under reflux with stirring for 6 h, then concentrated under vacuum and left to attain room temperature. The separated solid product was filtered, washed with water, dried and crystallized from an appropriate solvent (Table 5).

IR (cm^{-1}), **4a**: 1632 (C=N). IR (cm^{-1}). ^{1}H NMR ($CDCl_3$), **4a**: δ 3.34 (t, 2H, J = 12 Hz, SCH_2), 4.48 (t, 2H, J = 12 Hz, NCH_2), 7.32–7.67 (m, 10H, phenyl-H), 8.89 (s, 1H, pyrazole-C_5 H).

Table 4
Minimal inhibitory concentrations (MIC μg/ml) of test compounds.

Test compound	*E. coli*	*S. aureus*	*C. albicans*
4a	100	50	>200
4b	50	>200	>200
6a	50	25	>200
6b	>200	100	>200
8a	25	50	>200
8b	25	25	>200
10a	25	12.5	>200
10b	12.5	12.5	>200
Ampicillin	25	12.5	–
Clotrimazole	–	–	12.5

IR (cm^{-1}), **4b**: 1636 (C=N). ^{1}H NMR ($CDCl_3$), **4b**: δ 2.36 (s, 3H, CH_3), 3.37 (t, 2H, J = 12 Hz, SCH_2), 4.46 (t, 2H, J = 12 Hz, NCH_2), 7.32–7.64 (m, 5H, phenyl-H), 7.71 (d, 2H, J = 7.78 Hz, tolyl-$C_{3,5}$H), 7.84 (d, 2H, J = 7.78 Hz, tolyl-$C_{2,6}$H), 8.87 (s, 1H, pyrazole-C_5 H).

*5.1.4. 3-Aryl-1-phenyl-4-(4-fluorobenzyliminomethyl)-1H-pyrazole (**5a**,**b**)*

A solution of the appropriate aldehyde **1a**,**b** (10 mmol) in ethanol was added to an equivalent amount of 4-fluorobenzylamine (1.25 g, 10 mmol). The reaction mixture was heated under reflux for 4 h, concentrated and left to attain room temperature. The separated solid product was filtered, washed with ethanol, dried and crystallized from proper solvent (Table 5).

IR (cm^{-1}), **5a**: 1638, 1632 (C=N). IR (cm^{-1}). ^{1}H NMR ($CDCl_3$), **5a**: δ 4.37 (s, 2H, NCH_2), 7.14 (d, 2H, J = 7.64 Hz, fluorophenyl-$C_{2,6}$H), 7.33–7.68 (m, 12H, fluorophenyl-$C_{3,5}$H and phenyl-H), 8.18 (s, 1H, CHN), 8.91 (s, 1H, pyrazole-C_5 H). IR (cm^{-1}), **5b**: 1637, 1630 (C=N). ^{1}H NMR ($CDCl_3$), **5b**: δ 2.36 (s, 3H, CH_3), 4.38 (s, 2H, NCH_2), 7.16 (d, 2H, J = 7.64 Hz, fluorophenyl-$C_{2,6}$H), 7.27-7.69 (m, 7H, fluorophenyl-$C_{3,5}$H and phenyl-H), 7.72 (d, 2H, J = 7.78 Hz, tolyl-$C_{3,5}$H), 7.85 (d, 2H, J = 7.78 Hz, tolyl-$C_{2,6}$H), 8.21 (s, 1H, CHN), 8.88 (s, 1H, pyrazole C_5 H).

*5.1.5. 2-(3-Aryl-1-phenyl-1H-pyrazole-4-yl)-3-(4-fluorobenzyl)-4-oxo-thiazolidine (**6a**,**b**)*

Few crystals of anhydrous zinc chloride and thioglycolic acid (0.11 g, 12 mmol) were added to a solution of the selected Schiff's base **5a**,**b** (10 mmol) in anhydrous dimethylformamide (10 ml). The

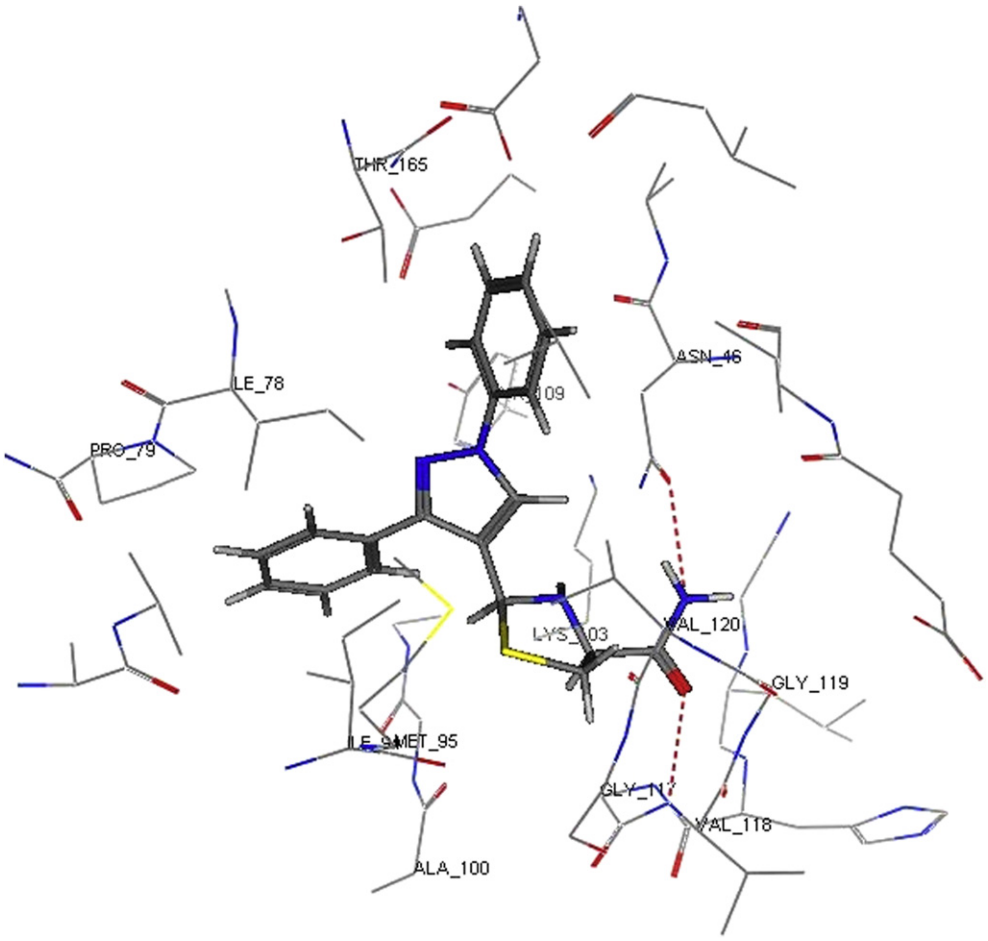

Fig. 6. 3D View from a molecular modeling study, of the minimum-energy structure of the complex of **10a** docked in DNA-gyrase B (PDB ID: 1EI1). Viewed using Molecular Operating Environment (MOE) module.

reaction mixture was heated under reflux for 8 h, cooled, and then poured into ice-cold water (50 ml). The separated solid was filtered, washed with water, dried and crystallized from aqueous ethanol (Table 5).

IR (cm^{-1}), **6a**: 1682 (C═O), 1634 (C═N). ^{1}H NMR ($CDCl_3$), **6a**: δ 3.72 (2d, 2H, J = 10 Hz, thiazol-C_5H) 4.48 (s, 2H, NCH_2), 5.69 (s, 1H, thiazol-C_2H), 7.13 (d, 2H, J = 7.64 Hz, fluorophenyl-$C_{2,6}$H), 7.31–7.69 (m, 12H, fluorophenyl-$C_{3,5}$H and phenyl-H), 8.91 (s, 1H, pyrazole-C_5 H). ^{13}C NMR ($CDCl_3$), **6a**: 34.2, 46.7, 48.3, 115.8, 117.6, 120.7, 123.4, 126.8, 127.9, 128.9, 129.2, 129.4, 129.8, 132.5, 133.4, 139.9, 150.2, 161.5, 171.8.

IR (cm^{-1}), **6b**: 1684 (C═O), 1637 (C═N). ^{1}H NMR ($CDCl_3$), **6b**: δ 2.34 (s, 3H, CH_3), 3.68 (2d, 2H, J = 10 Hz, thiazol-C_5H) 4.51 (s, 2H, NCH_2), 5.71 (s, 1H, thiazol-C_2H), 7.16 (d, 2H, J = 7.64 Hz, fluorophenyl-$C_{2,6}$H), 7.28–7.66 (m, 7H, fluorophenyl-$C_{3,5}$H and phenyl-H), 7.73 (d, 2H, J = 7.78 Hz, tolyl-$C_{3,5}$H), 7.82 (d, 2H, J = 7.78 Hz, tolyl-$C_{2,6}$H), 8.89 (s, 1H, pyrazole-C_5 H). ^{13}C NMR ($CDCl_3$), **6b**: 24.5, 34.3, 46.5, 48.6, 115.7, 117.6, 121.1, 123.6, 126.7, 127.6, 129.3, 129.7, 130.1, 130.3, 132.6, 138.6, 139.8, 150.4, 161.8, 172.1.

*5.1.6. (2RS,4R)-2-(3-Aryl-1-phenyl-1H-pyrazole-4-yl)-3-(ter-butyloxycarbonyl)-thiazolidine-4-carboxylic acid (**7a**,**b**)*

L-Cysteine (1.21 g, 10 mmol) and selected pyrazole aldehyde **1a**,**b** were suspended in 60% aqueous ethanol (20 ml) and the mixture was heated under reflux for 5 h, then cooled and concentrated under vacuum. The resulted slurry was treated with 2 N NaOH (6 ml) and $(Boc)_2O$ (2.34 g, 11 mmol) in 5 ml dioxane. After stirring for 5 h at room temperature, the reaction mixture was diluted with water and washed with ether (2 × 15 ml). The aqueous phase was acidified with crystalline citric acid and extracted by ethyl acetate (3 × 15 ml). The combined organic extract was evaporated under vacuum and the residue was crystallized from an appropriate solvent (Table 5).

IR (cm^{-1}), **7a**: 3378 (br., OH), 1734 (C═O), 1708 (C═O), 1632 (C═N), 1210, 1135 (C–O–C). IR (cm^{-1}). ^{1}H NMR ($CDCl_3$), **7a**: δ 1.39 (s, 9H, 3 (CH_3)), 3.21–3.78 (m, 2H, thiazol-C_5H), 4.50 (t, J = 7.80 Hz, 1H, thiazol-C_4H), 6.07 (s, 0.5H, thiazol-C_2H), 6.17 (s, 0.5H, thiazol-C_2H), 7.32–7.71 (m, 10H, phenyl-H), 8.87 (s, 1H, pyrazole-C_5 H).

IR (cm^{-1}), **7b**: 3372 (br., OH), 1732 (C═O), 1712 (C═O), 1635 (C═N), 1205, 1138 (C–O–C). ^{1}H NMR ($CDCl_3$), **7b**: δ 1.40 (s, 9H, 3 (CH_3)), 2.33 (s, 3H, CH_3), 3.22–3.76 (m, 2H, thiazol-C_5H), 4.53 (t, J = 7.80 Hz, 1H, thiazol-C_4H), 6.05 (s, 0.5H, thiazol-C_2H), 6.15 (s, 0.5H, thiazol-C_2H), 7.32–7.68 (m, 5H, phenyl-H), 7.71 (d, 2H, J = 7.78 Hz, tolyl-$C_{3,5}$H), 7.80 (d, 2H, J = 7.78 Hz, tolyl-$C_{2,6}$H), 8.90 (s, 1H, pyrazole-C_5 H).

*5.1.7. (2RS,4R)-2-(3-Aryl-1-phenyl-1H-pyrazole-4-yl)thiazolidine-4-carboxylic acid (**8a**,**b**)*

Anisole (1.1 ml, 10.4 mmol) was added at 0 °C to a solution of **7a**,**b** (5.2 mmol) in 4 N HCl/dioxane (10 ml). The reaction mixture was stirred for 1 h at room temperature. The solvent was removed *in vacuo* at room temperature, ether was added, and then the mixture was centrifuged. The obtained solid product was crystallized from a proper solvent (Table 5).

IR (cm^{-1}), **8a**: 3363 (br., OH), 3158 (NH), 1716 (C═O), 1637 (C═N). IR (cm^{-1}). ^{1}H NMR ($CDCl_3$), **7a**: δ 3.24–3.76 (m, 2H, thiazol-C_5H), 4.48 (t, J = 7.80 Hz, 1H, thiazol-C_4H), 6.05 (s, 0.5H, thiazol-C_2H), 6.16

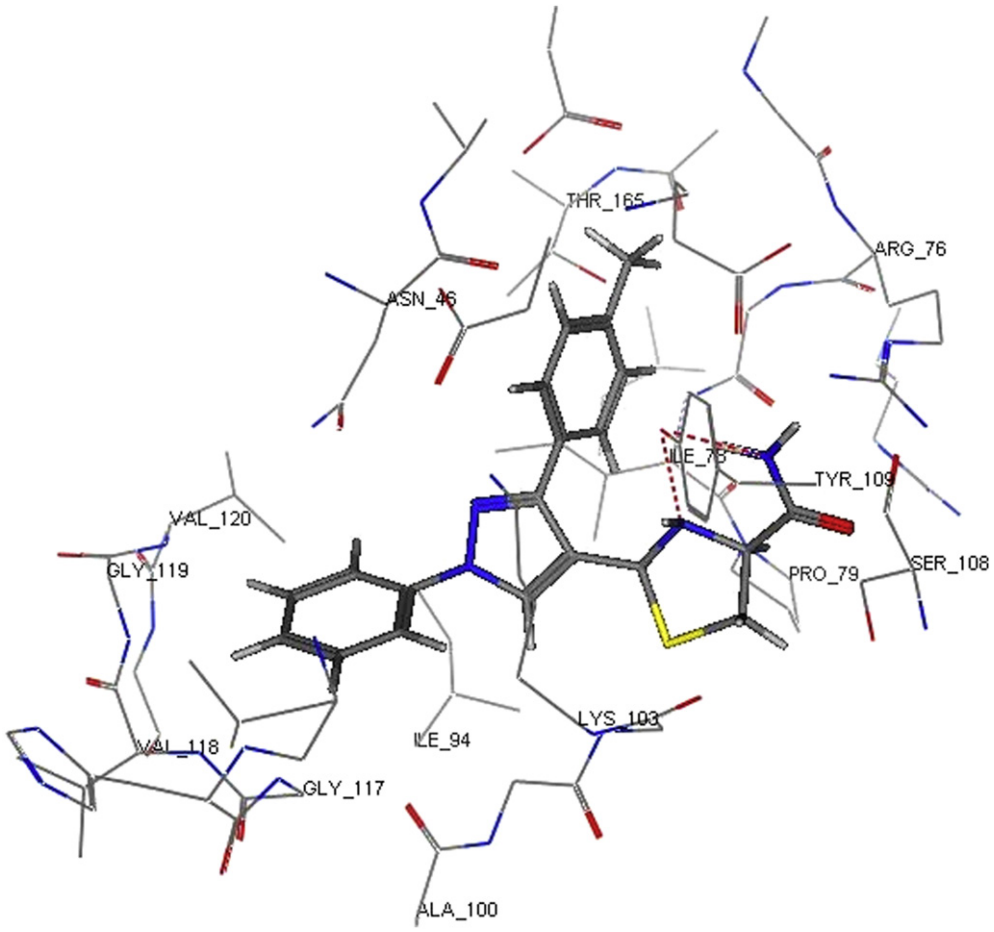

Fig. 7. 3D View from a molecular modeling study, of the minimum-energy structure of the complex of **10b** docked in DNA-gyrase B (PDB ID: 1EI1). Viewed using Molecular Operating Environment (MOE) module.

(s, 0.5H, thiazol-C_2H), 7.35–7.74 (m, 10H, phenyl-H), 8.84 (s, 1H, pyrazole-C_5 H). ^{13}C NMR ($CDCl_3$), **8a**: 35.6, 60.4, 65.2, 117.5, 120.1, 123.3, 126.2, 127.6, 128.7, 129.2, 129.6, 133.4, 140.1, 150.3, 175.2.

IR (cm^{-1}), **8b**: 3368 (br., OH), 3154 (NH), 1714 (C=O), 1631 (C=N). ^1H NMR ($CDCl_3$), **7b**: δ 2.31 (s, 3H, CH_3), 3.25–3.73 (m, 2H, thiazol-C_5H), 4.52 (t, J = 7.80 Hz, 1H, thiazol-C_4H), 6.07 (s, 0.5H, thiazol-C_2H), 6.16 (s, 0.5H, thiazol-C_2H), 7.33–7.69 (m, 5H, phenyl-H), 7.31 (d, 2H, J = 7.78 Hz, tolyl-$C_{3,5}H$), 7.82 (d, 2H, J = 7.78 Hz, tolyl-$C_{2,6}H$), 8.89 (s, 1H, pyrazole-C_5 H). ^{13}C NMR ($CDCl_3$), **8b**: 24.7, 35.4, 60.3, 65.4, 117.3, 120.4, 123.3, 126.0, 127.5, 129.4, 129.6, 130.3, 138.2, 139.7, 150.5, 174.8.

5.1.8. (2RS,4R)-2-(3-Aryl-1-phenyl-1H-pyrazole-4-yl)-3-(ter-butyloxycarbonyl)-thiazolidine-4-carboxamide (*9a*,*b*)

To a solution of the selected acid **7a**,**b** (10 mmol) in DMF (15 ml); HOBT·H_2O (1.84 g, 12 mmol) and DCC·HCl (2.48 g, 12 mmol) were added while stirring at 0 °C, and the mixture was further stirred at 0 °C for 1 h. Ammonium hydroxide solution (28%, 1.56 ml,40 mmol) was added and the mixture was stirred over night at room temperature. The mixture was filtered, the filtrate was evaporated under vacuum, and the residue was crystallized from an appropriate solvent (Table 5).

IR (cm^{-1}), **9a**: 3352, 3194 (NH_2), 1736 (C=O), 1682 (C=O), 1633 (C=N), 1211, 1138 (C–O–C). ^1H NMR ($CDCl_3$), **9a**: δ 1.41 (s, 9H, 3 (CH_3)), 3.21–3.75 (m, 2H, thiazol-C_5H), 4.55 (t, J = 7.80 Hz, 1H, thiazol-C_4H), 6.07 (s, 0.5H, thiazol-C_2H), 6.16 (s, 0.5H, thiazol-C_2H), 7.28–7.74 (m, 10H, phenyl-H), 8.31 (br. s, 2H, NH_2, D_2O exchangeable), 8.89 (s, 1H, pyrazole-C_5 H).

IR (cm^{-1}), **9b**: 3349, 3187 (NH_2), 1735 (C=O), 1684 (C=O), 1634 (C=N), 1208, 1136 (C–O–C). ^1H NMR ($CDCl_3$), **9b**: δ 1.40 (s, 9H, 3 (CH_3)), 2.35 (s, 3H, CH_3), 3.22–3.76 (m, 2H, thiazol-C_5H), 4.52 (t, J = 7.80 Hz, 1H, thiazol-C_4H), 6.06 (s, 0.5H, thiazol-C_2H), 6.16 (s, 0.5H, thiazol-C_2H), 7.33–7.71 (m, 5H, phenyl-H), 7.72 (d, 2H, J = 7.78 Hz, tolyl-$C_{3,5}H$), 7.81 (d, 2H, J = 7.78 Hz, tolyl-$C_{2,6}H$), 8.29 (br. s, 2H, NH_2, D_2O exchangeable), 8.91 (s, 1H, pyrazole-C_5 H).

5.1.9. (2RS,4R)-2-(3-Aryl-1-phenyl-1H-pyrazole-4-yl)thiazolidine-4-carboxamide (*10a*,*b*)

Anisole (1.1 ml, 10.4 mmol) was added at 0 °C to a solution of **9a**,**b** (5.2 mmol), in 4 N HCl/dioxane (10 ml) and the reaction mixture was stirred for 1 h at room temperature. The solvent was removed *in vacuo* at room temperature, ether was added, and the mixture was centrifuged. The obtained solid product was crystallized from a proper solvent (Table 5).

IR (cm^{-1}), **10a**: 3344, 3186, 3158 (NH_2, NH), 1686 (C=O), 1632 (C=N). ^1H NMR ($CDCl_3$), **10a**: δ 3.21–3.77 (m, 2H, thiazol-C_5H), 4.48 (t, J = 7.80 Hz, 1H, thiazol-C_4H), 6.09 (s, 0.5H, thiazol-C_2H), 6.15 (s, 0.5H, thiazol-C_2H), 7.33–7.73 (m, 11H, NH, phenyl-H), 8.29 (br. s, 2H, NH_2, D_2O exchangeable), 8.86 (s, 1H, pyrazole-C_5 H). ^{13}C NMR ($CDCl_3$), **10a**: 36.1, 60.2, 71.6, 117.4, 120.1, 123.3, 126.6, 127.4, 128.7, 129.2, 129.6, 133.2, 140.1, 149.7, 177.8.

IR (cm^{-1}), **10b**: 3339, 3192, 3166 (NH_2, NH), 1683 (C=O), 1635 (C=N). ^1H NMR ($CDCl_3$), **10b**: δ 2.35 (s, 3H, CH_3), 3.23–3.74 (m, 2H, thiazol-C_5H), 4.55 (t, J = 7.80 Hz, 1H, thiazol-C_4H), 6.07 (s, 0.5H, thiazol-C_2H), 6.16 (s, 0.5H, thiazol-C_2H), 7.31–7.68 (m, 6H, NH, phenyl-H), 7.73 (d, 2H, J = 7.78 Hz, tolyl-$C_{3,5}H$), 7.82 (d, 2H,

Table 5
Physical and analytical data of compounds **2**–**10**.

Comp. No.	R	Yield %	MP (°C)	Mol. Formula	Elemental analysis %, Calcd/Found			
			Cryst. Solvent	(Mol. wt)	C%	H%	N%	S%
2a	H	83	243–241	$C_{16}H_{13}N_3O$	**72.99**	**4.94**	**15.96**	
			(EtOH)	(263.29)	72.64	5.11	16.21	
2b	CH_3	84	258–259	$C_{17}H_{15}N_3O$	**73.67**	**5.45**	**15.15**	
			(EtOH)	(277.32)	73.42	5.61	14.92	
3a	H	85	252–254	$C_{16}H_{11}N_3$	**78.35**	**4.52**	**17.13**	
			(EtOH)	(245.27)	78.51	4.29	16.92	
3b	CH_3	82	262–264	$C_{17}H_{13}N_3$	**78.74**	**5.05**	**16.20**	
			(EtOH)	(259.30)	8.92	4.83	15.89	
4a	H	72	266–268	$C_{18}H_{15}N_3S$	**70.79**	**4.95**	**13.76**	**10.50**
			(EtOH/H_2O)(6:1)	(305.34)	70.92	5.16	13.85	10.21
4b	CH_3	76	273–275	$C_{19}H_{17}N_3S$	**71.44**	**5.36**	**13.15**	**10.04**
			(EtOH/H_2O)(6:1)	(319.42)	71.62	5.53	12.87	9.84
5a	H	72	259–260	$C_{23}H_{18}FN_3$	**77.73**	**5.10**	**11.82**	
			(EtOH/H_2O)(6:1)	(355.40)	77.52	4.92	12.01	
5b	CH_3	77	268–269	$C_{24}H_{20}FN_3$	**78.03**	**5.46**	**11.37**	
			(EtOH/H_2O)(6:1)	(369.41)	77.86	5.28	11.57	
6a	H	84	279–281	$C_{25}H_{20}FN_3OS$	**69.91**	**4.69**	**9.78**	**7.47**
			(EtOH/H_2O)(6:1)	(429.51)	70.15	4.38	9.92	7.61
6b	CH_3	89	291–293	$C_{26}H_{22}FN_3OS$	**70.41**	**5.00**	**9.47**	7.23
			(EtOH/H_2O)(6:1)	(443.53)	70.64	4.78	9.28	6.92
7a	H	87	257–258	$C_{24}H_{25}N_3O_4S$	**63.84**	**5.58**	**9.31**	7.10
			(ethyl acetate/n-hexane) (1:1)	(451.54)	63.62	5.21	9.53	6.86
7b	CH_3	85	284–185	$C_{25}H_{27}N_3O_4S$	**64.50**	**5.85**	**9.03**	**6.89**
			ethyl acetate/n-hexane) (1:1)	(465.56)	64.80	5.59	8.87	7.01
8a	H	73	250–252	$C_{19}H_{17}N_3O_2S$	**64.94**	**4.88**	**11.96**	**9.12**
			ethyl acetate/n-hexane) (1:1)	(351.42)	65.22	4.61	12.18	8.81
8b	CH_3	76	268–269	$C_{20}H_{19}N_3O_2S$	**65.73**	**5.24**	**11.50**	**8.77**
			ethyl acetate/n-hexane) (1:1)	(365.45)	65.50	5.52	11.28	8.98
9a	H	81	285–286	$C_{24}H_{26}N_4O_3S$	**63.98**	**5.82**	**12.44**	**7.12**
			(EtOH/H_2O)(6:1)	(450.55)	64.24	5.68	12.65	6.87
9b	CH_3	77	291–292	$C_{25}H_{28}N_4O_3S$	**64.63**	**6.07**	**12.06**	**6.90**
			(EtOH/H_2O)(5:1)	(464.58)	64.37	6.32	11.84	7.20
10a	H	75	257–258	$C_{19}H_{18}N_4OS$	**65.12**	**5.18**	**15.99**	**9.15**
			(EtOH/H_2O)(6:1)	(350.44)	64.86	4.92	16.21	9.42
10b	CH_3	76	276–278	$C_{20}H_{20}N_4OS$	**65.91**	**5.53**	**15.37**	**8.80**
			(EtOH/H_2O)(6:1)	(364.14)	66.23	5.78	15.12	8.51

J = 7.78 Hz, tolyl-$C_{2,6}$H), 8.30 (br. s, 2H, NH_2, D_2O exchangeable), 8.89 (s, 1H, pyrazole-C_5 H). ^{13}C NMR ($CDCl_3$), **10b**: 24.6, 36.3, 59.8, 71.3, 117.5, 120.3, 123.1, 126.4, 127.5, 129.4, 129.7, 130.3, 138.2, 139.8, 149.5, 177.5.

5.2. Anti-inflammatory activity

5.2.1. Cotton pellet-induced granuloma bioassay

Adult male Sprague–Dawley rats (120–140 g) obtained from Medical Research Institute, Alexandria University. The rats were acclimated one week prior to use and allowed unlimited access to standard rat chow and water. Prior to the start of experiment, the animals were randomly divided into groups of six rats each. Cotton pellet (35 ± 1 mg) cut from dental rolls were impregnated with 0.2 ml (containing 10 μmol) of a solution of the test compound in chloroform and the solvent was allowed to evaporate. Each cotton pellet was subsequently injected with 0.2 ml of an aqueous solution of antibiotics (1 mg penicillin G and 1.3 mg dihydrostreptomycin/ml). Two pellets were implanted subcutaneously, one in each axilla of the rat, under mild general anesthesia. One group of animals received the standard reference indomethacin and the antibiotics at the same level. Pellets containing only the antibiotics were similarly implanted in the control rats. Seven days later, the animals were sacrificed and the two cotton pellets, with adhering granulomas, were removed, dried for 48 h at 60 °C and weighed. The increment in dry weight (difference between the initial and final weights) was taken as a measure of granuloma. This was calculated for each group and the percentage reduction in dry weight of granuloma from control value was also calculated. The ED_{50} values were determined through dose response curves using doses of 4, 7, 10 and 15 μmol for each compound.

5.3. Carrageenan-induced rat paw edema

Male albino rats weighing 120–150 g (Medical Research Institute, Alexandria University) were used throughout the work. They were kept in the animal house under standard conditions of light and temperature with free access to food and water. The animals were randomly divided into groups of six rats each. The paw edema was induced by subplantar injection of 50 μl of 2% carrageenan in saline solution (0.9%). Indomethacin and the test compounds were dissolved in DMSO and were injected subcutaneously in a dose of 10 μmol/kg body weight, 1 h prior to carrageenan injection. Control group was injected with DMSO only. The volume of paw edema (ml) was determined by means of plethysmometer immediately after injection of carrageenan and 4 h later. The increase in paw volume between time 0 and 4 h was measured as described earlier [27]. The percentage protection against inflammation was calculated as follows:

$$\frac{V_c - V_d}{V_c} \times 100$$

where V_c is the increase in paw volume in the absence of test compound (control) and V_d is the increase in paw volume after injection of the test compound. Data were expressed as the mean ± SEM. Significant difference between the control and the

treated groups was performed using one way ANOVA. The difference in the means was considered significant at $P < 0.001$ using Tukey's multiple comparison test. The anti-inflammatory activity of the test compounds relative to that of indomethacin was also calculated.

5.4. Human COX-1 and COX-2 enzymatic assay

Human COX-1 and COX-2 activities were determined according to Wakitani et al. [40]. Human COX-1 (0.3 mg protein/assay) or COX-2 (1 mg protein/assay) was suspended in 0.2 ml of 100 mmol Tris/HCl buffer (pH 8) containing hematin (2 mmol) and tryptophan (5 mmol) as cofactors. The reaction mixture was pre-incubated with each test compound individually for 5 min at 24 °C. [^{14}C]-Arachidonic acid (100.00 dpm, 30 mmol) was added to the mixture and then incubated for 2 min (for COX-1) or 45 min (for COX-2) at 24 °C. The reaction was stopped by addition of 400 μl of a solution composed of Et_2O/MeOH/1 M Citric acid (30:4:1, v/v/v). After centrifugation of the mixture at 1700 × g for 5 min at 4 °C, 50 μl of the upper phase was applied to a thin layer chromatography plate. Thin layer chromatography was performed at 4 °C with solvent system consisting of Et_2O/MeOH/AcOH (90:2:0.1, v/v/v). Enzyme activity was calculated from the percent conversion of arachidonic acid to PGH2 and its decomposition products, using radiometric photographic system. The concentration of the compound causing 50% inhibition (IC_{50}) was calculated.

5.5. Ulcerogenic effects

The most active compounds **8b**, **10a** and **10b** were evaluated for their ulcerogenic potential in rats. Indomethacin was used as reference standard. Male albino rats (100–120 g) were fasted for 12 h prior to administration of the compounds. Water was given *ad libitum*. The animals were divided into groups of six rats each. Control group received 1% gum acacia orally. Other groups received indomethacin or test compounds orally in two equal doses at 0 and 12 h for three successive days at a dose of 30 μmol/kg body weight per day. Animals were sacrificed by diethyl ether 6 h after the last dose and the stomach was removed. An opening at the greater curvature was made and the stomach was cleaned by washing with cold saline and inspected with a 3X magnifying lens for any evidence of hyperemia, hemorrhage, definite hemorrhagic erosion or ulcer. An arbitrary scale was used to calculate the ulcer index which indicates the severity of stomach lesions. The percentage ulceration for each group was calculated as follows:

$$\%\ \text{Ulceration} = \frac{\text{Number of animals bearing ulcer in a group}}{\text{Total number of animals in the same group}} \times 100$$

5.6. Acute toxicity

The oral acute toxicity of compounds **8b**, **10a** and **10b** was investigated using male mice (20 g each, Medical Research Institute, Alexandria University) according to previously reported methods. The animals were divided into groups of six mice each. The compounds were given orally, suspended in 1% gum acacia, in doses of 1, 5, 10, 50, 150 mg/kg. The mortality percentage in each group was recorded after 24 h. Additionally the test compounds were investigated for their parenteral acute toxicity in groups of mice of six animals each. The compounds or their vehicle, propylene glycol (control), were given by intraperitoneal injection in doses of 5, 10, 20, 40, 80 mg/kg. The percentage survival was followed up to 7 days [21].

5.7. Docking studies

Computer simulated docking experiments were carried out under an MMFF94X force field in (PDB ID: 1CX2) using chemical computing group's Molecular Operating Environment (MOE-Dock 2005) software, Montréal, Canada.

5.8. Docking of human COX-2

The coordinate from the X-ray crystal structure of human COX-2 used in this simulation was obtained from the Protein Data Bank (PDB ID: 1CX2), where the selective COX-2 inhibitor **SC-588** is bound to the active site. The ligand molecules were constructed using the builder module and were energy minimized. The active site of COX-2 was generated using the MOE-Alpha Site Finder, and then ligands were docked within this active site using the MOE-Dock. The lowest energy conformation was selected and the ligand interactions (hydrogen bonding and hydrophobic interaction) with COX-2 were determined.

5.9. Docking of DNA-gyrase B

The coordinate from the X-ray crystal structure of DNA-gyrase B used in this simulation was obtained from the Protein Data Bank (PDB ID: 1EI1). The ligand molecules were constructed using the builder module and were energy minimized. The active site of DNA-gyrase B was generated using the MOE-Alpha Site Finder, and then ligands were docked within this active site using the MOE-Dock. The lowest energy conformation was selected and the ligand interactions (hydrogen bonding and hydrophobic interaction) with DNA-gyrase B were determined.

5.10. Antimicrobial activity

The micro-dilution susceptibility test in Müller-Hinton Broth (oxoid) and Sabouraud Liquid Medium (oxoid) were used for determination of antibacterial and antifungal activities. Test organisms were *E. coli* (*E. coli*) ATCC 25922 as an example of Gram-negative bacteria, *S. aureus* (*S. aureus*) ATCC 19433 as an example of Gram-positive bacteria and *C. albicans* (*C. albicans*) as yeast like fungus. Ampicillin trihydrate and clotrimazole were used as standard antibacterial and antifungal agents, respectively. Solutions of the test compounds, ampicillin trihydrate and clotrimazole were prepared in DMSO at concentration of 1600 μg/ml. From this stock solution, two-fold dilutions of the compounds (800, 400, … 6.25 μg/ml) were inoculated to the corresponding wells. Plates were incubated at 36 °C for 24–48 h, with the incubation chamber kept sufficiently humid. At the end of the incubation period, the minimal inhibitory concentrations (MIC) were determined. Controls with DMSO and uninoculated media were run parallel to the test compounds under the same conditions.

References

[1] J.M. Scheiman, Clin. Update 12 (2005) 1–4.
[2] S. Fiorucci, L. Santucci, E. Distrutti, Dig. Liver Dis. 39 (2007) 1043–1051.
[3] D.C. Kosegarten, E.F. LaSala, S.F. Long, in: L. Shargel, A.H. Mutnick, P.F. Souney, L.N. Swanson, L.H. Block (Eds.), Comprehensive Pharmacy Review, Lippincott Williams and Wilkins, Philadelphia, 2001, pp. 289–291.
[4] M.R. Griffin, A. Yared, W.A. Ray, Am. J. Epidemiol. 151 (2000) 488–496.
[5] Y. Song, D.T. Connor, R. Doubleday, R.J. Sorenson, A.D. Sercel, P.C. Unangst, B.D. Roth, R.B. Gilbertsen, K. Chan, D.J. Schrier, A. Guglietta, D.A. Bornemeier, R.D. Dyer, J. Med. Chem. 42 (1999) 1151–1160.

[6] N.V. Chandrasekharan, H. Dai, K.L. Turepu Roos, N.K. Evanson, J. Tomsik, T.S. Elton, D.L. Simmons, PNAS 99 (2002) 13926–13931.
[7] A. Palomer, F. Cabre, J. Pascual, J. Campos, M.A. Trujillo, A. Entrena, M.A. Gallo, L. Garcia, D. Mauleon, A. Espinosa, J. Med. Chem. 45 (2002) 1402–1411.
[8] B.P. Bandgar, S.S. Gawande, R.G. Bodade, N.M. Gawande, C.N. Khobragade, Bioorg. Med. Chem. 17 (2009) 8168–8173.
[9] S.V. Bhandari, S.C. Dangre, K.G. Bothara, A.A. Patilm, A.P. Sarkate, D.K. Lokwani, S.T. Gore, B.J. Deshmane, V.T. Raparti, C.V. Khachane, Eur. J. Med. Chem. 44 (2009) 4622–4636.
[10] P.D. Sauzem, S. Sant'Anna Gda, P. Machado, M.M. Duarte, J. Ferreira, C.F. Mello, P. Beck, H.G. Bonacorso, N. Zanatta, M.A. Martins, M.A. Rubin, Eur. J. Pharmacol. 616 (2009) 91–100.
[11] M.A. Chowdhury, K.R. Abdellatif, Y. Dong, D. Das, M.R. Suresh, E.E. Knaus, J. Med. Chem. 52 (2009) 1525–1529.
[12] S. Khode, V. Maddi, P. Aragade, M. Palkar, P.K. Ronad, S. Mamledesai, A.H. Thippeswamy, D. Satyanarayana, Eur. J. Med. Chem. 44 (2009) 1682–1688.
[13] S.G. Kucukguzel, S. Rollas, H. Erdeniz, M. Kiraz, A.C. Ekinci, A. Vidin, Eur. J. Med. Chem. 35 (2000) 761–771.
[14] M.J. Genin, D.A. Allwine, D.J. Anderson, M.R. Barbachyn, D.E. Emmert, S.A. Garmon, D.R. Graber, K.C. Grega, J.B. Hester, D.K. Hutchinson, J. Morris, R.J. Reischer, C.W. Ford, G.E. Zurenko, J.C. Hamel, R.D. Schaadt, D. Stapert, B.H. Yagi, J. Med. Chem. 43 (2000) 953–970.
[15] A. Tanitame, Y. Oyamada, K. Ofuji, Y. Kyoya, K. Suziki, H. Ito, M. Kawasaki, K. Nagai, M. Wachi, J. Yamagishi, Bioorg. Med. Chem. Lett. 14 (2004) 2857–2862.
[16] A. Tanitame, Y. Oyamada, K. Ofuji, K. Suziki, H. Ito, M. Kawasaki, M. Wachi, J. Yamagishi, Bioorg. Med. Chem. Lett. 14 (2004) 2863–2866.
[17] A. Tanitame, Y. Oyamada, K. Ofuji, M. Fujimoto, N. Iwai, Y. Hiyama, K. Suziki, H. Ito, H. Terauchi, M. Kawasaki, K. Nagai, M. Wachi, J. Yamagishi, J. Med. Chem. 47 (2004) 3693–3696.
[18] A.M. Farghaly, A.A. Bekhit, J.Y. Park, Arch. Pharm. Pharm. Med. Chem. 333 (2000) 53–57.
[19] A.A. Bekhit, H.T.Y. Fahmy, Sh.A.F. Rostom, A.M. Baraka, Eur. J. Med. Chem. 38 (2003) 27–36.
[20] A.A. Bekhit, H.T.Y. Fahmy, Arch. Pharm. Pharm. Med. Chem. 336 (2003) 111–118.
[21] A.A. Bekhit, T. Abdel-Azeim, Bioorg. Med. Chem. 12 (2004) 1935–1945.
[22] A.A. Bekhit, Egyptian Patent, Appl. No. 465 9, 2007.
[23] A.A. Bekhit, Egyptian Patent, Appl. No. 1117 12, 2003.
[24] A.A. Bekhit, H.M.A. Ashour, A. Guemei, Arch. Pharm. Chem. Life Sci. 338 (2005) 167–174.
[25] A.A. Bekhit, H.M. Abdel-Rahman, A. Guemei, Arch. Pharm. Chem. Life Sci. 339 (2006) 81–87.
[26] A.A. Bekhit, H.M.A. Ashour, A.E. Bekhit, H.M. Abdel-Rahman, S.A. Bekhit, J. Enzy. Inhibit. Med. Chem. 24 (2009) 296–309.
[27] A.A. Bekhit, H.M.A. Ashour, Y.S. Abdel Ghany, A.E. Bekhit, A. Baraka, Eur. J. Med. Chem. 43 (2008) 456–463.
[28] A.A. Bekhit, H.M.A. Ashour, A.E. Bekhit, S.A. Bekhit, Med. Chem. 5 (2009) 103–117.
[29] S.A.F. Rostom, I.M. El-Ashmawy, Abd H.A. El Razik, M.H. Badr, H.M.A. Ashour, Bioorg. Med. Chem. 17 (2009) 882–895.
[30] S.K. Bharti, G. Nath, R. Tilak, S.K. Singh, Eur. J. Med. Chem. 45 (2010) 651–660.
[31] N.P. Rai, T.D. Venu, B.K. Manuprasad, S. Shashikanth, P.N. Arunachalam, A. Firdouse, Chem. Biol. Drug Des. 75 (2010) 400–406.
[32] M. Bernard, E. Hulley, H. Molenda, K. Stochla, U. Wrzeciono, Pharmazie 41 (1986) 560–562.
[33] E. Pretsch, P. Bühlmann, C. Affolter (Eds.), Structure Determination of Organic Compounds, Springer-Verlag, Berlin, Heidelberg, New York, 2000, p. 212 Chapter 5.
[34] R. Caujolle, J.D. Favrot, P.R. Loiseau, M. Payard, H. Amarouch, H. Lazrek, M.D. Linas, J.P. Seguela, P.M. Loiseau, C. Bories, P. Gavral, Pharm. Acta Helv. 66 (1991) 237–240.
[35] G.S. Sheppard, D. Pireh, G.M. Carrera, M.G. Bures Jr., H.R. Heyman, D.H. Steinman, S.K. Davidsen, J.G. Phillips, D.E. Guinn, P.D. May, R.G. Conway, D.A. Rhein, W.C. Calhoun, D.H. Albert, T.J. Magoc, G.W. Carter, J.B. Summers, J. Med. Chem. 37 (1994) 2011–2032.
[36] M. Bodanszky, A. Bodanszky (Eds.), The Practice of Peptide Synthesis, Springer-Verlag, Berlin, 1994, p. 20.
[37] R. Faggiani, H.E. Howard-Lock, C.J.L. Lock, R. Orgias, Can. J. Chem. 69 (1991) 1–7.
[38] R. Meier, W. Schuler, P. Desaulles, Experientia 6 (1950) 469–471.
[39] M. Di Rosa, D.A. Willoughby, J. Pharm. Pharmcol. 23 (1971) 297–298.
[40] K. Wakitani, T. Nanayama, M. Masaki, M. Matsushita, Jpn. J. Pharmacol. 78 (1998) 365–371.
[41] S. Hammarström, P. Falardeau, PNAS 74 (1997) 3691–3695.
[42] M.S. Abou Zeit-Har, T. Verimer, J.P. Long, Pharmazie 37 (1982) 593–595.
[43] M. Verma, M. Tripathi, A.K. Saxena, K. Shanker, Eur. J. Med. Chem. 29 (1994) 941–946.
[44] Molecular Operating Environment (MOE) version. Chemical Computing Group, Inc, Montréal, Canada, 2006–08. http://www.chemcomp.com.
[45] R.G. Kurumbail, A.M. Stevens, J.K. Gierse, J.J. McDonald, R.A. Stegeman, J.Y. Pak, D. Gildehaus, J.M. Iyashiro, T.D. Penning, K. Seibert, P.C. Iscekson, W.C. Stallings, Nature 384 (1996) 644–648.
[46] P.R. Murray, E.J. Baron, M.A. Pfaller, F.C. Tenover, R.H. Yolken, Manual of clinical microbiology. in: G.L. Woods, J.A Washington (Eds.), Antimicrobial Agents and Susceptibility Testing, Am. Soc. Mircobiol., 1995 Washington, DC.
[47] K. Sato, Y. Inoue, T. Fujii, H. Aoyama, M. Inoue, S. Mitsuhashi, Antimicrob. Agents Chemother. 30 (1986) 777–780.